Electronic and vibrational properties of ultrathin SiO$_2$ films grown on Mo(112)

S. Wendt, E. Ozensoy, T. Wei, M. Frerichs, Y. Cai, M. S. Chen, and D. W. Goodman*

Department of Chemistry, Texas A & M University, College Station, Texas 77842-3012, USA

(Received 2 November 2004; revised manuscript received 4 May 2005; published 7 September 2005)

Ultrathin SiO$_2$ films on Mo(112) were synthesized using different preparation procedures and characterized with ultraviolet photoelectron spectroscopy (UPS), metastable impact electron spectroscopy (MIES), and polarization modulation infrared reflection absorption spectroscopy (PM-IRAS). By correlating the vibrational and electronic data, an assignment of the prominent spectral features are made. The physical properties of SiO$_2$ films near one monolayer are influenced by the Mo substrate due to the Si-O-Mo linkages, whereas films greater than two monolayers show properties comparable to bulklike silica samples. The electronic and vibrational properties of the SiO$_2$ thin films are strongly coverage dependent. The data show that highly ordered SiO$_2$ films can be grown up to one monolayer, whereas films with a thickness of greater than one monolayer are amorphous.

I. INTRODUCTION

In recent years, ultrathin oxide films grown on metal substrates have attracted considerable interest.[1–8] The morphology and electronic properties of the films as a function of thickness and the detailed structure of the substrate-oxide interface are important issues relevant to semiconductor manufacturing. In addition, there is significant interest in growing well-defined oxide layers as a support for model heterogeneous catalysts. Due to efficient charge transport through the ultrathin films, electron- or ion-based surface analytical probes can be used for surface characterization without the usual charging problems typically encountered for insulating bulk oxides.[9–12] In this paper the epitaxial growth and thermal stability of oxide films synthesized and characterized under ultrahigh vacuum (UHV) conditions are described.

Although stoichiometric SiO$_2$ films on Mo substrates have been previously prepared under UHV, their lack of crystallinity make them less than ideal model catalyst supports.[13] However recently, well-ordered, ultrathin silica films have been grown on a Mo(112) substrate.[14–20] These SiO$_2$ thin films have been characterized with surface analytical techniques including scanning tunneling microscopy (STM),[15,19,20] UPS,[15,17,18] IRAS,[15] x-ray photoelectron spectroscopy (XPS),[14,20] low-energy electron diffraction (LEED),[14–16] spot-profile analyzing low-energy electron diffraction (SPALEED),[14,15] and high resolution electron energy loss spectroscopy (HREELS).[16]

Although various methods for preparing SiO$_2$ films on Mo(112) have been used in earlier studies, there is general agreement that surface imperfections, e.g. defect density, are considerably reduced by annealing the films at elevated temperatures. A sharp $c(2 \times 2)$ LEED pattern from the annealed SiO$_2$ films on Mo(112) is an important consequence of annealing and indicative of a highly ordered film.[14–16] Ordering of the SiO$_2$ films upon annealing at high temperatures has been verified by STM,[15,19] IRAS,[15] HREELS,[16] and MIES/UPS.[17,18]

In previous reports on the valence electronic structure of thin, well-ordered SiO$_2$ films on Mo(112), it has been suggested, based on Auger electron spectroscopy (AES)/UPS[15] and MIES/UPS,[17,18] that these systems closely simulate the electronic properties of bulk silica. Well-resolved features in the valence band of SiO$_2$/Mo(112) that appear after annealing between 1150 and 1250 K have been interpreted as due to the high degree of order in the SiO$_2$ films.[15,17,18]

The HREELS spectrum of a SiO$_2$ film with a coverage of one monolayer (ML) is characterized by a feature at ~ 1048 cm^{-1}, assigned to the asymmetric Si-O stretch mode of Si-O-Mo linkages.[16] Based on this assignment, well-ordered SiO$_2$ films on Mo(112) have been described as a Mo(112)-$c(2 \times 2)$-[SiO$_4$] surface where all four oxygen atoms of the [SiO$_4$] tetrahedron are connected directly to the Mo substrate atoms.[16] It is noteworthy that the IRAS data of Schroeder *et al.* show a sharp feature at ~ 1048 cm^{-1}, however, the thickness of the films in this study is purported to be 2 ML rather than 1 ML.[15]

The nature of the SiO$_2$/Mo(112) system is still a subject of active scientific debate, and various structural models have been proposed.[16,21] In this paper we focus on the synthesis and characterization of ultrathin SiO$_2$ films grown on Mo(112) using various preparation methods. Electronic and vibrational properties of the SiO$_2$ films can be best explained in terms of the coverage of the films. At film thicknesses of one monolayer or less, the electronic and vibrational properties of the film are markedly influenced by the Mo substrate due to extensive Si-O-Mo linkages.

II. EXPERIMENTAL

The experiments were carried out in two UHV surface analysis chambers that are equipped with AES, LEED, and a quadrupole mass spectrometer (QMS). The addendum chamber for PM-IRAS studies is equipped with CaF$_2$ windows. The PM-IRAS data were acquired with a Bruker Equinox 55 infrared spectrometer at 8 min/spectrum with 8 cm^{-1} resolution at an angle of 85° from the surface normal. Details of the apparatus as well as the operational principles of the PM-IRAS technique are described elsewhere.[19,22–26]

Electronic spectroscopic experiments were performed in a second chamber equipped with a cold-cathode gas discharge source producing both ultraviolet photons (He I: $E^* = 21.2$ eV) and metastable He $2\,^3$S($E^* = 19.8$ eV) atoms with thermal kinetic energy.[27] The axis of the double-pass cylindrical mirror analyzer (CMA) is perpendicular to the incoming photon/metastable beam. MIES and UPS spectra were acquired with photon/metastable beams incident at 48° with respect to the surface normal. The MIES and UPS spectra were measured simultaneously using a mechanical chopper (time-of-flight method).[27] The resolution of the analyzer, estimated from the width of the Fermi edge, is ~0.3 eV. Work functions were estimated from the low-energy onset of the secondary electrons in the UPS spectra that were acquired with a bias voltage applied between the analyzer and the sample.

For wide bandgap materials or metals with work functions lower than ~3.5 eV, He* atoms deexcite at the surface via Auger deexcitation (AD). In this case, a plot of the intensity of the ejected electrons versus their kinetic energies yields the surface density of states (SDOS) for the topmost layer of the surface.[28,29] In the spectra reported here, the intensities are plotted as a function of binding energy (E_B). The fermi level (E_F) of the Mo substrate was used as the reference in all of the UPS and MIES spectra ($E_B = 0$).

For all SiO$_2$ thin films considered, AES data were collected concomitant to the UPS/MIES and PM-IRAS measurements. For films of ~1 ML thickness, the prominent features in the AES spectra are the transitions at 187 eV (MNV) and at 223 eV (MVV) of Mo. The feature at 78 eV due to the Si LVV of SiO$_2$[30] is less intense than the MNV and MVV features of Mo in both experimental setups, and becomes dominant only for films with $\theta \geq 1.5$ ML. The attenuation of the Mo MNV (187 eV) feature[31] was used as a measure of the film thickness "t." The formula,

$$t = \ln(I_0/I) \times \lambda \times \cos(\alpha),$$

was applied, with I_0 and I being the peak intensities of the Mo MNV (187 eV) feature prior to and after SiO$_2$ film growth, respectively. Since a CMA was used, the angle α between the sample normal and the detected Auger electrons was ~42°. A mean-free path (λ) of 0.95 nm for the 187 eV electrons in SiO$_2$ was used.[32]

The Mo(112) crystals were spot welded to U-shaped tantalum wires for resistive heating. The sample temperature could be varied from 90 K (by cooling with liquid N$_2$) to 1300 K (by resistive heating) and to 2200 K (by e-beam heating); the temperature was measured by a (W-5%Re/W-26%Re) thermocouple spot welded to the backside of the sample. The Mo(112) crystals were cleaned by multiple flashes to 2100 K and the cleanliness verified with AES.

III. RESULTS

A. Multistep SiO$_2$ film synthesis on Mo(112)

The first method utilized in the current work to synthesize SiO$_2$ thin films on Mo(112) follows the recipe of Chen *et al.*[16] In this method (method 1), the Mo(112) substrate was
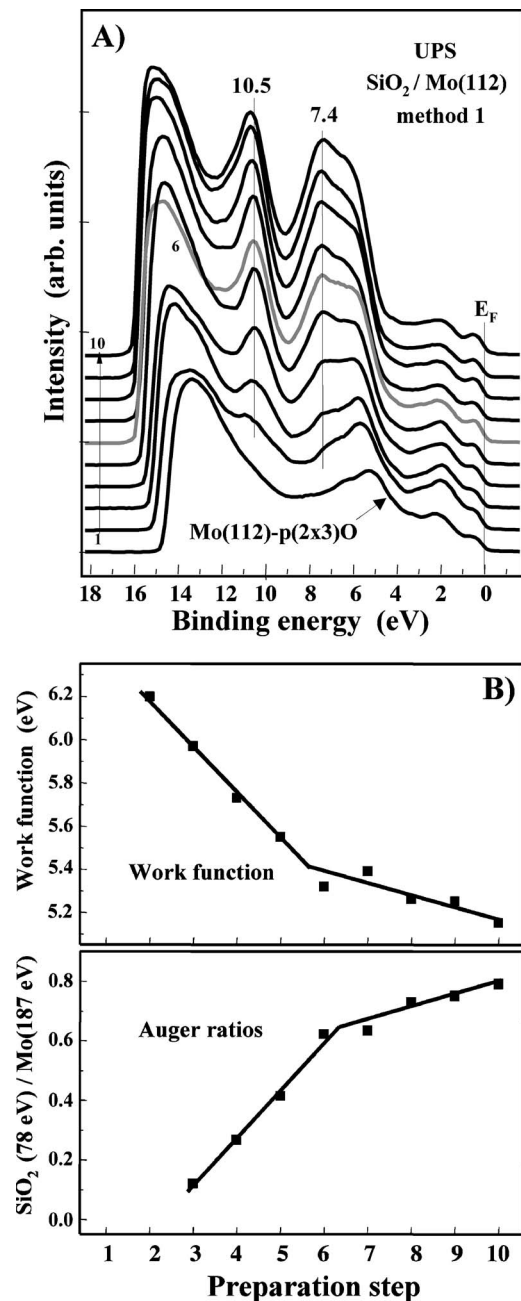

FIG. 1. (a) UPS spectra illustrating the step-by-step preparation of SiO$_2$/Mo(112) (method 1). Spectrum (6) (thick grey curve) corresponds to the 1 ML film. (b) Upper panel: work function data estimated from the spectra shown in (a); lower panel: AES ratios corresponding to the ten preparation steps.

first exposed to oxygen (5×10^{-8} Torr) at 850 K for ~10 min to produce a $p(2 \times 3)$O surface reconstruction.[33] Subsequently, small amounts of Si were deposited, with each deposition step followed by an anneal at 800 K in an oxygen atmosphere for 5 min, then the temperature increased to 1200 K for an additional 5 min. During the annealing process the oxygen pressure was kept at 1×10^{-7} Torr. These Si deposition and annealing steps were repeated several times until a coverage of 1 ML was achieved.
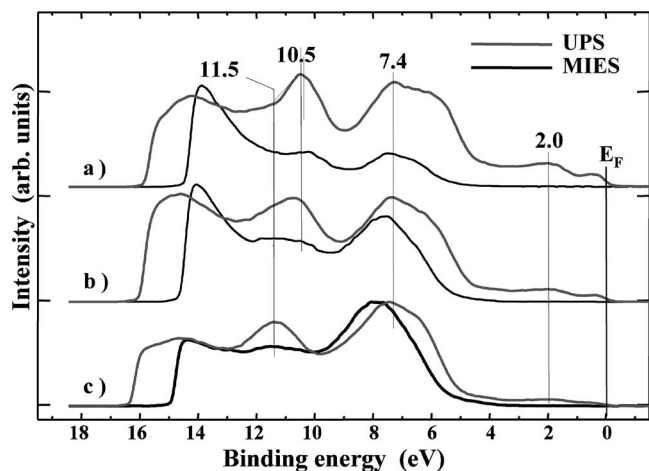
Method 1 synthesis was followed with UPS (Fig. 1(a))

FIG. 2. Selected UPS and MIES spectra illustrating the growth of an amorphous silica film on top of a well-ordered SiO_2 thin film: (a) $SiO_2/Mo(112)$ surface prepared by method 1 ($\sim$1 ML); (b) after 4 additional deposition/oxidation cycles ($\sim$1.4 ML); and (c) after a total of 16 deposition/oxidation cycles ($\sim$2.6 ML). During the additional oxidation cycles, each 10 min, the sample temperature was 850 K.

and AES (Fig. 1(b)) measurements. Spectrum (1) in Fig. 1(a) is that of the Mo(112)-$p(2 \times 3)$O surface that exhibit dominant features between 4 and 7 eV and less intense states near E_F.[34] The structure between 4 and 7 eV results from the interaction of O(2p) electrons with Mo spd hybridized states that are energetically close to the Fermi edge.[35] After depositing Si and annealing, spectrum (2) show an O(2p) band with enhanced intensity and a new band at $\sim$10.5 eV. An increase in the film coverage leads to an increase of both bands. Based on previous reports, the band between 5 and 9 eV corresponds to O(2p) nonbonding states of SiO_2.[36–42] The band at $\sim$10.5 eV is in the region of the Si-O bonding states;[36–42] its position and intensity will be discussed below. Spectrum (6) in Figure 1(a) is attributed to a 1 ML SiO_2 film given the appearance of the break points in the AES ratios and in the work function data (Fig. 1(b)). The corresponding thickness of the film at this point in the synthesis procedure is estimated to be $\sim$0.4 nm, consistent with a coverage of 1 ML. It is noteworthy that this surface exhibits a sharp $c(2 \times 2)$ LEED pattern.

Figure 2 summarizes the UPS and MIES data acquired for SiO_2 films with coverages >1 ML prepared by using the 1 ML preparation described above and increasing the coverage using successive Si deposition and oxidation cycles. Only small quantities were deposited and subsequently oxidized at 850 K to prepare stoichiometric SiO_2 films. Therefore, many deposition/oxidation cycles had to be performed to increase the coverage sufficiently. For the 1 ML film, the maximum of the Si-O bonding feature is at $\sim$10.5 eV in UPS and MIES (curves (a)). After increasing the coverage to $\sim$1.4 ML (curves (b)), the bonding feature is at $\sim$10.8 eV, with a shoulder at $\sim$11.5 eV. At higher coverages, i.e., at $\sim$2.6 ML (curves (c)), the bonding band is most intense at $\sim$11.5 eV. Note that this thick silica film is essentially stoichiometric, since almost no states in the bandgap region are detectable, even with MIES.[17,18] In the corresponding AES spectrum, no
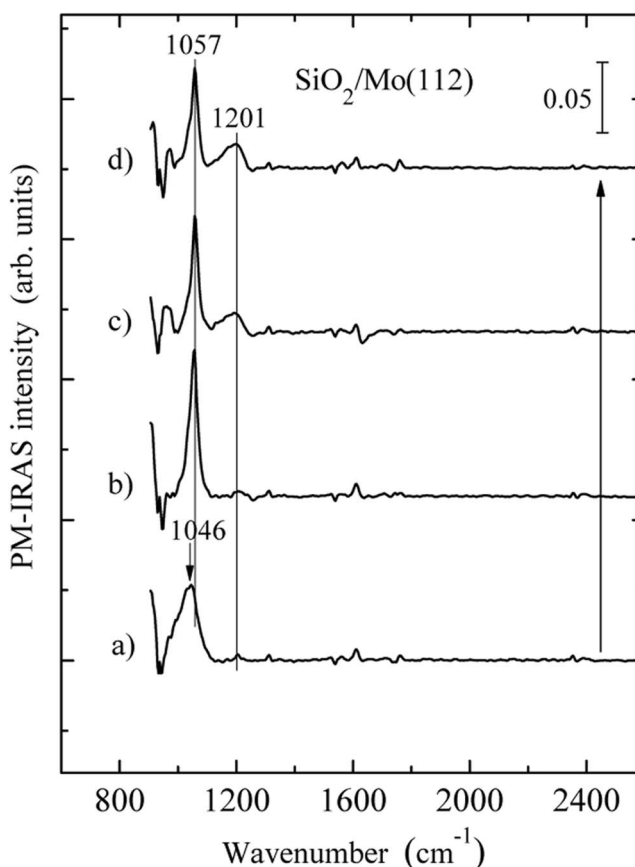

FIG. 3. A series of PM-IRAS spectra collected during step-by-step preparation of SiO_2 films on Mo(112). Films (a) and (b) were prepared using anneals at 800 and 1200 K (method 1) while the additional oxidation cycles to produce films (c) and (d) were performed at 800 K. The coverages of SiO_2 estimated from the AES data are (a) $\sim$0.6 ML, (b) $\sim$1.0 ML, (c) $\sim$1.1 ML, and (d) $\sim$1.2 ML.

Si^0 feature at $\sim$90 eV was detected, supporting this conclusion. A diffuse $c(2 \times 2)$ LEED pattern with a relatively high background was obtained for this surface.

Experiments similar to those summarized in Fig. 2 were carried out using PM-IRAS (Fig. 3). Starting with film (a) in the submonolayer range ($\theta \sim 0.6$ ML), SiO_2 films corresponding to coverages of $\sim$1.0, $\sim$1.1, and $\sim$1.2 ML, were synthesized (curves (b)–(d)). Film (a) is characterized by a broadband at $\sim$1046 cm^{-1} (FWHM=84 cm^{-1}) with a shoulder on the low-frequency side at $\sim$980 cm^{-1}. At about $\sim$1 ML (film (b)), a significant sharpening of this single vibrational band is observed (FWHM=29 cm^{-1}) in addition to a minor blue shift to $\sim$1057 cm^{-1}. Other important aspects of the spectrum for film (b) are the symmetry of the feature at $\sim$1057 cm^{-1} and the disappearance of the shoulder at $\sim$980 cm^{-1}. For coverages above 1 ML (films (c) and (d)), the feature at 1057 cm^{-1} remains very sharp, although slightly attenuated in intensity. In addition, a new feature at $\sim$1201 cm^{-1} is apparent in the spectra of the films with $\theta > 1$ ML, which is asymmetric on the low-frequency side with a shoulder at $\sim$1170 cm^{-1}. With increasing coverage, the intensity of the feature at 1201 cm^{-1} increases.
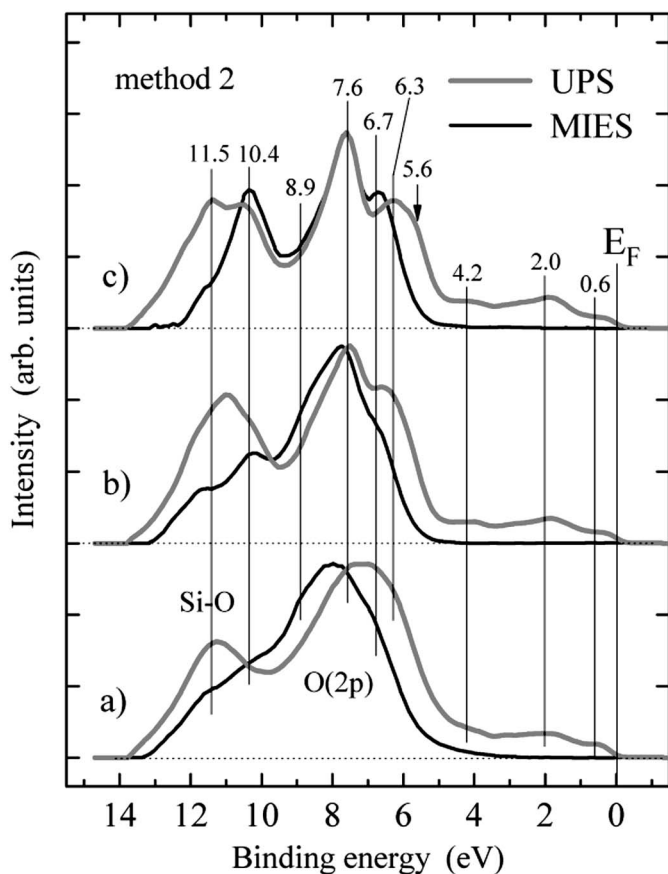
FIG. 4. (a) A comparison of SiO$_2$ thin films prepared by method 2. The UPS/MIES spectra in (a) correspond to an amorphous SiO$_2$ film of ~1.8 ML thickness that was prepared by oxidation at 800 K for 20 min. The spectra in (b) were obtained from a SiO$_2$ film (~1.7 ML), where a final anneal at 1100 K for 10 min was performed. (c) Spectra of a ~1.2 ML film that was prepared using a final anneal at 1150 K for 30 min. The contribution of secondary electrons was subtracted using an exponential approach. Spectra are normalized with respect to the maximum of the nonbonding band at ~7.6 eV.

B. Single-step SiO$_2$ film synthesis on Mo(112)

A second method (method 2) for SiO$_2$ film synthesis also begins with a Mo(112)-$p(2 \times 3)$O surface. However, in method 2, Si is deposited in a single step without intervening oxidizing cycles. The amount of Si deposited is typically that needed to synthesize 1.5–2 ML of SiO$_2$. The sample was oxidized via annealing at 800 K in an oxygen atmosphere ($p = 1 \times 10^{-7}$ Torr) for a minimum of 10 min. Finally, the sample was further annealed at 1050 K or, in certain cases, to 1150–1250 K, using the same oxygen pressure.

MIES and UPS data obtained for three films synthesized using method 2 are summarized in Fig. 4. Film (a) was prepared utilizing an oxidation step at 800 K for 20 min ($\theta \sim 1.8$ ML). The MIES spectrum of this film shows a broad O(2p) band at ~8 eV and smaller contributions due to Si-O bonding states at ~10.4 and ~11.5 eV. In UPS, the two bands appear at ~7 and ~11.4 eV, respectively, while states originating from the substrate are seen between 0 and 5 eV. With the exception of these Mo states, the UPS and
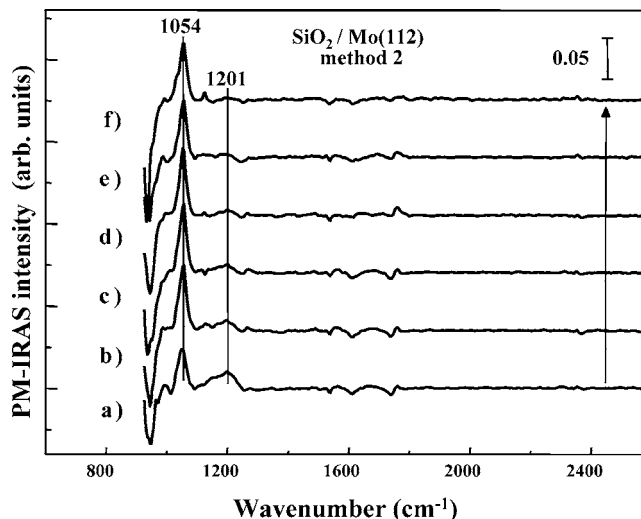

FIG. 5. Series of high-temperature annealing experiments performed on a SiO$_2$ film prepared by method 2: (a) ~1.3 ML SiO$_2$ film after oxidation at 850 K; (b)–(f) SiO$_2$ films after annealing at 1140, 1150, and 1200 K for durations of 10–25 min in the presence of oxygen ($p = 1 \times 10^{-7}$ Torr).

MIES spectra of film (a) resemble those obtained for a-SiO$_2$ grown on various Si substrates.[36,37] Films (b) and (c) in Fig. 4 were prepared by anneals at 1100 K (10 min) and 1150 K (30 min), respectively, leading to SiO$_2$ films with coverages of ~1.7 ML and ~1.2 ML, respectively. The O(2p) nonbonding band of film (c) shows a fine structure consisting of two features at ~7.6 and ~6.7 eV, and ~7.6 and ~6.3 eV in MIES and UPS, respectively. Furthermore, the relative contribution of the feature at ~10.5 eV is enhanced in comparison to films (a) and (b). The latter is more obvious in MIES than in UPS. The appearance of the fine structure for film (c) is accompanied by an increase of the states of the Mo substrate near to E_F in UPS. Furthermore, there is a shoulder at ~5.6 eV apparent in the UPS spectrum that is not evident in the other UPS spectra. The $c(2 \times 2)$ LEED pattern of film (c) is very sharp, indicating a high ordered surface.

PM-IRAS was also used to investigate the SiO$_2$ films synthesized with method 2 (Fig. 5). Starting with a ~1.3 ML SiO$_2$ film (a), silica films (b)–(f) were prepared by successive annealing cycles in the presence of 1×10^{-7} Torr O$_2$ at 1140, 1150, and 1200 K for 10 to 25 min. The striking decrease in the intensity of the band at ~1201 cm^{-1} during annealing is accompanied by the sharpening and growth of the feature at ~1057 cm^{-1}. Finally, after five successive annealing steps, film (f) with $\theta \sim 1.0$ ML is produced. The film thickness was verified by AES and its order, by a sharp $c(2 \times 2)$ LEED pattern.

For reference, a much thicker SiO$_2$ film was grown by Si deposition in the presence of O$_2$ using the procedure of Xu and Goodman.[13] This recipe was used to grow a ~4.8 ML amorphous SiO$_2$ film on Mo(112) (Fig. 6(a)). Next, the coverage of this amorphous film was reduced by annealing at 1250 K. Comparing the spectrum of film (a) with those of films (b) and (c), it is apparent that the broad asymmetric band at 1165 cm^{-1} becomes sharper due to annealing at
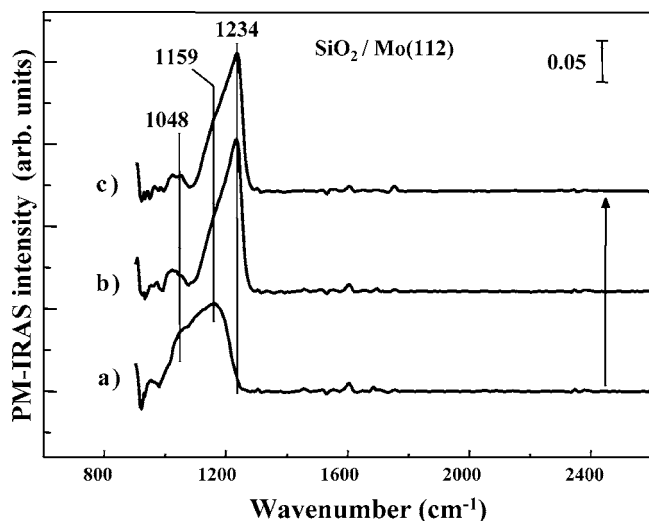
FIG. 6. High-temperature annealing experiments performed on an a-SiO_2 film prepared by Si deposition in oxygen [$p(O_2)=2 \times 10^{-5}$ Torr]: (a) As-grown a-SiO_2 film with a coverage of ~4.8 ML; (b) up to ~3.6 ML; and (c) up to ~3.0 ML, respectively, reduced SiO_2 films. The temperature during annealing was 1250 K and a pressure of $p(O_2)=1 \times 10^{-7}$ Torr was used.

1250 K. Furthermore, the band shifts to 1234 cm^{-1}, forming a much more intense feature with a shoulder at 1159 cm^{-1}. In addition, a small feature at 1048 cm^{-1} is evident in all of the spectra of Fig. 6, although in film (a), this feature is convoluted with the broadband at 1159 cm^{-1}.

IV. DISCUSSION

A. PM-IRAS

SiO_2 films on various substrates have been studied extensively in the literature using vibrational spectroscopic techniques.[13,15,16,39,40,43–46] Our discussion of SiO_2 films on Mo(112) will focus primarily on the phonon structure between 1000 and 1400 cm^{-1}, i.e., the asymmetric stretching (AS) region, as the vibrational features corresponding to symmetric stretching (~768 cm^{-1}) and bending (~496 cm^{-1}) modes of SiO_2/Mo(112)[16] were not accessible due to the cutoff frequencies of the CaF$_2$ windows used in the experiments.

Amorphous SiO_2 films reveal typically two different asymmetric stretching modes: in-phase motion of adjacent O atoms (AS_1) and out-of-phase motion of adjacent O atoms (AS_2).[44] Since the optical phonon band is composed of transverse (TO) *and* longitudinal (LO) modes, four different AS vibrational features are observed in the IR spectra at ~1076 cm^{-1} (TO-AS_1), ~1160 cm^{-1} (LO-AS_2), ~1200 cm^{-1} (TO-AS_2), and ~1256 cm^{-1} (LO-AS_1).[44] However, the SiO_2 films studied in this work have thicknesses well below the so-called Berreman thickness.[45–47] Therefore TO modes are expected to be fully suppressed whereas LO modes corresponding to the interlinking of the [SiO_4] tetrahedra and other bands such as the ones corresponding to Si-O-Mo linkages of [SiO_4] tetrahedra to the metallic Mo(112) substrate are anticipated to be observable.[47] Conse-

quently, the vibrational features between 1100 and 1250 cm^{-1} are assigned to LO-AS_1 and LO-AS_2 modes of Si-O-Si linkages whereas vibrational features between 1000 and 1100 cm^{-1} are attributed to the Si-O-Mo linkages. Note that for SiO_2 films grown on a metal surface, the AS_1-LO mode was observed at a wide range, 1180–1250 cm^{-1}, depending on the annealing temperature,[13] 1190–1218 cm^{-1} as a function of the film thickness (within 3 ML).[15]

During the initial stages of the SiO_2 film growth on Mo(112) using method 1, only a single broad vibrational feature at ~1046 cm^{-1} is apparent (Fig. 3(a)). This feature is associated with the Si-O-Mo linkages of isolated [SiO_4] tetrahedra at the surface. That there is no evidence of an LO mode at 1100–1250 cm^{-1} at this coverage (0.6 ML) is consistent with there being no Si-O-Si linkages between these isolated [SiO_4] units.[16] In previous reports, a shoulder at ~980 cm^{-1}, similar to the one seen in Fig. 3(a), was attributed to suboxides in the SiO_2/Si interface[43] or to the presence of Si-OH groups on SiO_2/Mo(112).[15] However, after a high-temperature anneal, no OH-related stretching features were apparent. Therefore, the presence of Si-OH groups on SiO_2/Mo(112) can be ruled out, fully consistent with recent work addressing the interaction of water with SiO_2/Mo(112).[48] Furthermore, it is known from previous AES and XPS data that SiO_2 films grown on Mo(112) do not contain suboxides for coverages $\theta < 1$ ML.[14] Thus, the shoulder at ~980 cm^{-1} is likely due to oxygen atoms bonded to the Mo substrate. According to previous vibrational studies we assign the shoulder at ~980 cm^{-1} to the stretching mode [$\nu(Mo=O)$] of terminal atop oxygen on the topmost Mo atoms.[49–51] This assignment is consistent with the disappearance of the 980 cm^{-1} feature and the formation of a sharp and symmetric feature at ~1057 cm^{-1} upon the formation of a well-ordered SiO_2 film at 1 ML (Fig. 3(b)).

After completion of the monolayer film (Fig. 3(c)), the formation of a second and a relatively less ordered SiO_2 layer is observed. This is evident from the appearance of an asymmetric feature at ~1201 cm^{-1} with a shoulder at ~1170 cm^{-1} corresponding to LO modes of AS_1 and AS_2 for Si-O-Si linkages, respectively. The appearance of such LO modes after completion of the first layer suggests the formation of Si-O-Si linkages between the [SiO_4] tetrahedra initially disconnected at lower coverages.[16]

Figure 5 illustrates that method 2 also can be used to obtain a highly ordered SiO_2 film by annealing an amorphous >1 ML SiO_2 film in oxygen at elevated temperatures. The ordered film with a coverage close to one monolayer obtained at the end of these annealing steps shows only a single sharp vibrational feature at ~1054 cm^{-1} with a FWHM of ~29 cm^{-1}.

LO modes of bulklike SiO_2 can be addressed by growing relatively thick SiO_2 films where Si-O-Si linkages are known to exist between the [SiO_4] tetrahedra and shown to exhibit intense LO bands. Figure 6 presents such thick SiO_2 films grown on Mo(112) where LO modes are visible at ~1160 cm^{-1} (LO-AS_2) and ~1234 cm^{-1} (LO-AS_1). In addition to these bands, the feature at ~1048 cm^{-1} associated with Si-O-Mo linkages is evident in these spectra. It should be noted that the high-temperature annealing steps lead to

TABLE I. Energy positions of the valence orbitals for various SiO_2 films determined by MIES and UPS (He I). Binding energies and positions of the valence band edges are given with respect to E_F in eV. The estimated thicknesses are in Å. All listed figures refer to this work. In Ref. 36 it is not specified how the position of the Fermi level was estimated.

System	Thickness	Technique	E_{Si-O}	$E_{O(2p)}$	E_{VB}	Reference
$SiO_x/Si(111)$	6	UPS	10.7	6.6±1.4	5.2	Ishii *et al.*
		MIES	9.6/10.6	7.25±1.2	5.8	(Ref. 36)
Naturally oxidized	11	UPS	11.1	7.2±1.3	5.9	Brause *et al.*
Si(100)		MIES	10.3/11.5	7.5±1.2	6.2	(Ref. 37)
a-$SiO_2/Mo(112)$	8.5	UPS	11.4	6.3–8.4	5.8	Figure 2
		MIES	10.6/11.7	6.7–9.0	6.45	film (c)
a-$SiO_2/Mo(112)$	6	UPS	11.4	6.0–8.5	5.6	Figure 4
		MIES	10.4/11.6	6.7–9.3	6.4	film (a)
1 ML $SiO_2/Mo(112)$	3.5–4	UPS	10.5	5.6–7.9	5.15	Figure 2
method 1		MIES	10.4	6.6–8.0	6.2	film (a)
1.2 ML $SiO_2/Mo(112)$	4.5	UPS	10.5/11.4	6.0–8.3	5.6	Figure 4
method 2						film (c)
		MIES	10.4	6.5–8.3	6.25	

ordering of the SiO_2 films and to sharpening and growth of the LO-AS$_1$ band at ~1234 cm^{-1} with concurrent attenuation of the LO-AS$_2$ feature at ~1160 cm^{-1}. Similar intensity changes for LO-AS$_1$ and LO-AS$_2$ modes have been reported for thick SiO_2 films on Mo(110)[13] and for the transition from amorphous silicon dioxide to ordered α quartz.[44]

B. UPS and MIES

Likewise the electronic properties of SiO_2 films on various substrates have been addressed previously.[15,17,18,36–42] UPS has been frequently employed to study the valence band of various SiO_2 surfaces while MIES has been used to a lesser extent. For a comparison with previous work using these two spectroscopies,[36,37] we summarize in Table I the positions of the valence bands and the valence band edge. The relative band positions and the widths of the bands of the spectra in Refs. 36 and 37 agree very well. Deviations of the band positions with respect to E_F are due to an uncertainty in the assignment of the Fermi level in Ref. 36. Note that in the present work the valence band edge of the thick a-SiO_2 films agrees exactly with that reported by Brause *et al.* It is also noteworthy that all of the spectra are dominated by the O(2p) nonbonding band. The Si-O bonding bands are clearly less intense than the O(2p) nonbonding bands for both MIES and UPS.

Since the thicker SiO_2 films in the present work (Figs. 2(c) and 4(a)) show spectra very similar to those of various SiO_2 surfaces in the literature[36–42] it is appropriate to use these films as a reference where Si-O-Si linkages predominate. Therefore, the broad Si-O bonding feature with a maximum at ~11.5 eV is assigned to a surface consisting of Si-O-Si linkages. In contrast, the spectra observed for films of one monolayer that were prepared by method 1 (Figs. 1(a) and 2(a)) clearly differ from the spectra of the thicker films. This difference arises due to influence of the Mo substrate—a view consistent with the vibrational data ob-

tained using PM-IRAS (see previously) and HREELS.[16] Consequently, we attribute the sharp and intense Si-O bonding band at ~10.5 eV to Si-O-Mo linkages at the surface. This assignment is supported by the AES and work function data in Fig. 1(b), where break points indicate the completion of the first ML. It is noteworthy that the existence of Si-O-Mo linkages at the interface is also evident from XPS measurements.[14(a),20]

The results shown in Fig. 2 further support the assignment of the features at ~11.5 and ~10.5 eV to Si-O-Si and Si-O-Mo linkages, respectively. These results suggest that within the range of 1 to ~2.5 ML the band in the Si-O bonding region is a convolution of features at ~10.5 and ~11.5 eV. Since the second layer consists of Si-O-Si linkages, the maximum of the Si-O bonding band shifts to higher binding energies as the coverage is increased. At a coverage of ~2.6 ML, the contribution of the feature at ~10.5 eV is no longer obvious with either UPS or MIES. The states close to E_F are still detectable with UPS even for a thick SiO_2 film since this technique probes several layers in the near-surface region. According to the results shown in Fig. 2 we conclude that bulklike electronic properties of silica develop within the first 2 ML. These results are consistent with the suggested thickness lower limit of usable SiO_2 gate electric materials observed by Muller *et al.*[52] Based on EELS in a scanning transmission electron microscope these authors found the thinnest, usable SiO_2 film on a Si substrate to be ~0.7 nm.[52] It is also worth noting that a very similar result (2–3 ML) was obtained for MgO thin films on Ag(100) based on scanning tunneling spectroscopy (STS) studies in combination with UPS and EELS.[5]

The intense feature at ~10.5 eV for films with θ~1 ML (method 1) is linked to the sharing of O atoms at the SiO_2/Mo interface. Upon the formation of the interfacial bond, these O atoms likely accumulate electron density from adjacent Mo atoms, leading to the observed intense feature. That the energy position of this feature is altered with respect to that assigned to Si-O-Si linkages in SiO_2 films indicates
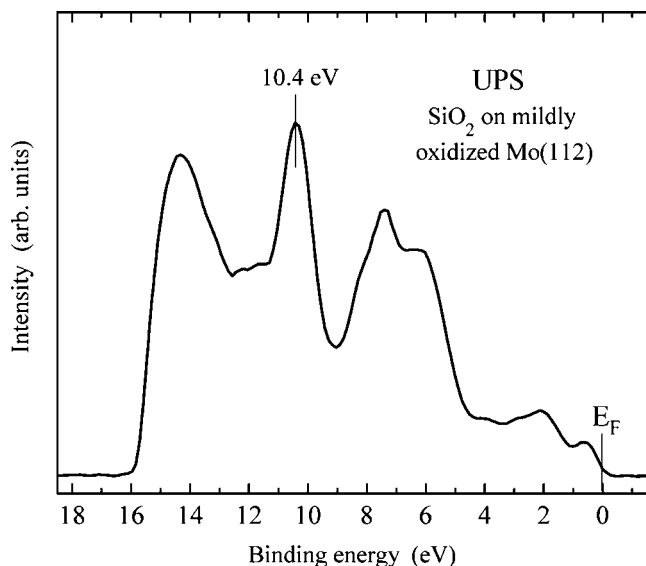
FIG. 7. UPS of a SiO$_2$ thin film ($\sim$1.1 ML) grown on a Mo(112) oxidized at 1000 K and an O$_2$ pressure of 1×10^{-7} Torr. Subsequently, Si was deposited in a single step and oxidized at 800 K followed by annealing in oxygen at 1050 K.

hybridization upon the formation of the interfacial bond. It is noteworthy that the intensity of the feature at $\sim$10.5 eV can be further enhanced by mild oxidization of the substrate prior to the SiO$_2$ film growth (Fig. 7). This result undoubtedly shows that the feature at $\sim$10.5 eV can only be explained invoking hybridization with states of the substrate. It appears that the intensity of the $\sim$10.5 eV feature can be used as a measure of the extent to which the substrate is involved, i.e., an intensity of this feature as high as that in Fig. 7 indicates that the substrate is partly oxidized. Note that temperatures as high as 1000 K are sufficient to oxidize various Mo samples.[31,35,49–51] Interestingly, UPS data reported by Schroeder *et al.* likewise show an intensive feature at $\sim$10.5 eV, although the SiO$_2$ films in this particular study were prepared by a procedure similar to method 2, but with a 1250 K anneal for 30 mins.[15]

When method 2 is used to prepare the SiO$_2$ thin films, a stoichiometric, but amorphous, SiO$_2$ film is formed after the first oxidation step at 800 K. Under these preparation conditions the coverage of the SiO$_2$ film is close to 2 ML, and hence the Si-O bonding feature appears near 11.5 eV (Fig. 4(a)). The appearance of the Si-O bonding feature at lower binding energies for films that were annealed at 1100 and 1150 K, respectively, indicates a reduction of the film thickness induced by the high-temperature anneal. This explanation is supported by AES data and the enhanced intensity of the features between 0 and 5 eV in UPS. The results in Fig. 4 suggest that the formation of a well-ordered SiO$_2$ film and the reduction of the film thickness occur simultaneously.

Next, we address the fine structure of the O(2p) nonbonding band that appears after annealing of SiO$_2$/Mo(112) in oxygen (method 2). Considering earlier UPS measurements regarding thermally grown, a-SiO$_2$ films[36–41] and α quartz,[42] the splitting in two well-resolved nonbonding features as evident for film (c) in Fig. 4, is unique. On the other hand, it has

been outlined that a splitting of the O(2p) nonbonding band is expected if the differently oriented O(2p) nonbonding orbitals are positioned with an angle of 90°.[38] This, however, is not valid for most silica polymorphs, suggesting that relatively less structured nonbonding bands as seen for a-SiO$_2$ are also expected for crystalline SiO$_2$ surfaces. That the latter is indeed likely the case can be concluded, considering quantum chemical calculations of the density of states (DOS).[53] Assuming that the surface density of states (SDOS) do not considerably differ from the DOS of the silica polymorphs, we conclude that the splitting of the nonbonding band into two features is unlikely caused by the transformation of the a-SiO$_2$ film into a crystalline film with the same thickness. Rather, we attribute the splitting of the nonbonding band to isolated [SiO$_4$] tetrahedral, attached with their O atoms to the substrate. In these isolated [SiO$_4$] tetrahedra the O(2p) nonbonding orbitals can be bent 90° away from each other, not the case for most other SiO$_2$ polymorphs. This interpretation is supported by the fact that the splitting of the nonbonding band is only evident for films with a coverage close to 1 ML, i.e., for film (c) in Fig. 4. Alternatively, there is the possibility that a closed, crystalline SiO$_2$ film of 1 ML thickness has formed after annealing a-SiO$_2$/Mo(112). Due to the variability in the bonding of SiO$_2$ with the Mo(112) substrate, the film could contain O(2p) nonbonding orbitals bent at a large angle with respect to each other. We do not rule out this possibility based on the MIES/UPS data of film (c) in Fig. 4, particularly since the UPS data exhibit features at $\sim$10.5 eV as well at $\sim$11.5 eV. This interpretation, however, of the fine structure in the O(2p) nonbonding region is inconsistent with the HREELS[16] and PM-IRAS data (see previous).

The proposed picture regarding the fine structure of the O(2p) nonbonding band after annealing is consistent with our previous interpretation with respect to defect sites.[17,18] A broad O(2p) band in MIES and UPS as found for thicker films indeed indicates a high density of extended defects as steps and corners since the films prepared by oxidation at 800 K are amorphous (method 2). Annealing at high temperatures leads to a reduction of the SiO$_2$ film thickness. As the film coverage approaches one monolayer, most [SiO$_4$] tetrahedra are attached via the O atoms to the Mo substrate. Since the less-ordered second layer is no longer present, a well-ordered film is produced with a low density of extended defects.

Different oriented O(2p) nonbonding orbitals at the surface are not only indicated by the splitting of the O(2p) band but also evident considering the differences between MIES and UPS spectra.[36] Orbitals that are aligned perpendicular to the surface appear intense in UPS as well as in MIES. In contrast, parallel or nearly parallel oriented O(2p) nonbonding orbitals appear much less intense in MIES than in UPS. This relates to the fact that UPS also probes deeper lying orbitals, whereas He* metastable atoms deexcite with a high probability on those O(2p) orbitals oriented perpendicular to the surface. Therefore, states between 5 and 7 eV seen with UPS are not apparent in the MIES spectrum (Figs. 2 and 4). This rationalization, which was first suggested by Ishii *et al.*,[36] holds also for the Si-O bonding orbitals. It explains why the Si-O bonding states are much more intense in UPS

than in MIES. Considering the different surface sensitivities, it is also understandable why the maximum of the nonbonding band in MIES and UPS coincides for thin SiO_2 films, yet differs for thicker, amorphous SiO_2 films.

Another interesting aspect regarding method 2 is the shoulder at ~5.6 eV evident on the low binding energy side in the UPS spectrum of film (c) in Fig. 4. This shoulder most likely arises from the hybridization of $O(2p)$ electrons at the interface. Note that the $O(2p)$ nonbonding states of pure silica overlap with the $O(2p)$ feature of the Mo(112)-$p(2 \times 3)$O surface. With respect to its energy position, it is difficult to assign this shoulder solely to SiO_2 states or whether other states, influenced by the Mo substrate, contribute to this shoulder. However, it is noteworthy that this shoulder is only resolved if the feature at ~10.5 eV is intense, i.e., subsequent to annealing in O_2 at high temperature.[54] In addition, if this shoulder were to correspond to pure $O(2p)$ states of silica, then it should be detected with MIES, which is not the case. Note that all purely SiO_2-derived features are detectable (although with different intensity) with both UPS and MIES. On the contrary, features originating from Mo or mixed states are not necessarily detectable with MIES. Furthermore, preparation method 1 results in an $O(2p)$ nonbonding feature broadened toward lower binding energies compared with method 2 (see E_{VB} in Table I). Altogether these results allow us to conclude that the shoulder at ~5.6 eV certainly does not originate solely from $O(2p)$ nonbonding states of SiO_2. Rather, this shoulder is likely due to the hybridization of states between the Mo substrate and $O(2p)$ nonbonding states of silica. As a result of the decrease in the SiO_2 film coverage, it is likely that a fraction of the Mo substrate becomes uncovered upon annealing at high temperatures and with the initiation of oxidation. If this is indeed the case, then the lower value of E_{VB} for method 1 indicates that the Mo substrate is, to a greater extent, oxidized when method 1 is used. Since the Mo substrate for method 2 is completely covered by Si and SiO_2 before annealing in oxygen at high temperatures, the substrate is better protected against oxidation than for method 1, where the substrate is only partly covered by SiO_2 after an anneal at 1200 K. In addition, initial oxidation of the substrate is likely responsible for a broad, less-structured $O(2p)$ nonbonding feature for films prepared using method 1, i.e., no separation of the nonbonding band is apparent, as seen for films prepared using method 2.

V. CONCLUSIONS

Ultrathin silica (SiO_2) films were prepared on a Mo(112) substrate utilizing different synthesis procedures. Regardless of the detailed preparation recipe, the electronic and vibrational properties of monolayer films can be best rationalized by a surface dominated by Si-O-Mo linkages. For SiO_2 films with coverages up to one monolayer, a single vibrational feature at 1048–1057 cm^{-1} is seen with PM-IRAS corresponding to Si-O-Mo linkages. The modes at 1201–1234 cm^{-1} and ~1160 cm^{-1} (LO-AS$_1$ and LO-AS$_2$) are only evident for films with coverages greater than one monolayer and are associated with the formation of Si-O-Si linkages in the second layer of the SiO_2 films. Completion of the first monolayer is also indicated by break points in the AES and work function data upon employing a step-by-step preparation method. The UPS spectra of the films prepared using a stepwise method show bands originating from $O(2p)$ nonbonding orbitals broadened toward lower binding energies, partially induced by initial oxidation of the Mo substrate. On the other hand, reduction of the coverage to approximately one monolayer by annealing a thick film in oxygen leads to a well-ordered SiO_2 film. In this well-ordered film the $O(2p)$ nonbonding band consists of two well-resolved features, consistent with two distinct $O(2p)$ nonbonding orbitals at the surface, suggesting a high degree of order of these monolayer SiO_2 films. Since the separation of the $O(2p)$ nonbonding band is linked to a coverage of one monolayer, we believe that the fine structure of the nonbonding band is attributed to isolated $[SiO_4]$ tetrahedra attached via O atoms to the substrate. Different orientations of $O(2p)$ nonbonding orbitals are also evident when comparing the intensities in MIES and UPS spectra. The data presented here support the previous assignment of Chen *et al.*, that the well-ordered structure of SiO_2 films on Mo(112) is restricted to the first monolayer.[16] For the complete development of bulk-like electronic properties, SiO_2 thin films with a thickness of ~2 ML are required.

---

*Author to whom correspondence should be addressed. Electronic address: goodman@mail.chem.tamu.edu

[1] D. A. Muller, D. A. Shashkov, R. Benedek, L. H. Yang, J. Silcox, and D. N. Seidman, Phys. Rev. Lett. **80**, 4741 (1998).

[2] S. Altieri, L. H. Tjeng, F. C. Voogt, T. Hibma, and G. A. Sawatzky, Phys. Rev. B **59**, R2517 (1999).

[3] S. Altieri, L. H. Tjeng, and G. A. Sawatzky, Phys. Rev. B **61**, 16948 (2000).

[4] H. L. Meyerheim, R. Popescu, J. Kirschner, N. Jedrecy, M. Sauvage-Simkin, B. Heinrich, and R. Pinchaux, Phys. Rev. Lett. **87**, 076102 (2001).

[5] S. Schintke, S. Messerli, M. Pivetta, F. Patthey, L. Libioulle, M. Stengel, A. De Vita, and W. D. Schneider, Phys. Rev. Lett. **87**, 276801 (2001).

[6] Y. T. Matulevich, T. J. Vink, and P. A. Zeiijlmans van Emmichoven, Phys. Rev. Lett. **89**, 167601 (2002).

[7] C. Lamberti, E. Groppo, C. Prestipiono, S. Casassa, A. M. Ferrari, C. Pisani, C. Giovanardi, P. Luches, S. Valeri, and F.

Boscherini, Phys. Rev. Lett. **91**, 046101 (2003).

[8] L. Savio, E. Celasco, L. Vattuone, M. Rocca, and P. Senet, Phys. Rev. B **67**, 075420 (2003).

[9] D. W. Goodman, J. Vac. Sci. Technol. A **14**, 1526 (1996).

[10] H.-J. Freund, H. Kuhlenbeck, and V. Steammler, Rep. Prog. Phys. **59**, 283 (1996).

[11] S. C. Street, C. Xu, and D. W. Goodman, Annu. Rev. Phys. Chem. **48**, 43 (1997).

[12] M. Bäumer and H.-J. Freund, Prog. Surf. Sci. **61**, 127 (1999).

[13] (a) X. Xu and D. W. Goodman, Appl. Phys. Lett. **61**, 774 (1992); (b) X. Xu and D. W. Goodman, Surf. Sci. **282**, 323 (1993).

[14] (a) T. Schroeder, A. Hammoudeh, M. Pykavy, N. Magg, M. Adelt, M. Bäumer, and H.-J. Freund, Solid-State Electron. **45**, 1471 (2001); (b) T. Schroeder, M. Adelt, B. Richter, M. Naschitzki, M. Bäumer, and H.-J. Freund, Surf. Rev. Lett. **7**, 7 (2000); (c) T. Schroeder, M. Adelt, B. Richter, M. Naschitzki, M. Bäumer, and H.-J. Freund, Microelectron. Reliab. **40**, 841 (2000).

[15] T. Schroeder, J. B. Giorgi, M. Bäumer, and H.-J. Freund, Phys. Rev. B **66**, 165422 (2002).

[16] M. S. Chen, A. K. Santra, and D. W. Goodman, Phys. Rev. B **69**, 155404 (2004).

[17] Y. D. Kim, T. Wei, and D. W. Goodman, Langmuir **19**, 354 (2003).

[18] S. Wendt, Y. D. Kim, and D. W. Goodman, Prog. Surf. Sci. **74**, 141 (2003).

[19] E. Ozensoy, B. K. Min, A. K. Santra, and D. W. Goodman, J. Phys. Chem. B **108**, 4351 (2004).

[20] B. K. Min, W. T. Wallace, and D. W. Goodman, J. Phys. Chem. B **108**, 14609 (2004).

[21] D. Ricci and G. Pacchioni, Phys. Rev. B **69**, 161307(R) (2004).

[22] E. Ozensoy, D. C. Meier, and D. W. Goodman, J. Phys. Chem. B **106**, 9367 (2002).

[23] B. J. Barner, M. J. Green, E. I. Saez, and R. M. Corn, Anal. Chem. **63**, 55 (1991), and references therein.

[24] G. A. Beitel, A. Laskov, H. Osterbeek, and E. W. Kuipers, J. Phys. Chem. **100**, 12494 (1996).

[25] (a) E. Ozensoy, C. Hess, and D. W. Goodman, J. Am. Chem. Soc. **124**, 8524 (2002); (b) E. Ozensoy and D. W. Goodman, Phys. Chem. Chem. Phys. **6**, 3765 (2004).

[26] C. Hess, E. Ozensoy, and D. W. Goodman, J. Phys. Chem. B **107**, 2759 (2003).

[27] (a) W. Maus-Friedrichs, M. Wehrhahn, S. Dieckhoff, and V. Kempter, Surf. Sci. **237**, 257 (1990); (b) W. Maus-Friedrichs, S. Dieckhoff, and V. Kempter, *ibid.* **249**, 149 (1991).

[28] Y. Harada, S. Masuda, and H. Ozaki, Chem. Rev. (Washington, D.C.) **97**, 1897 (1997).

[29] H. Morgner, Adv. At., Mol., Opt. Phys. **42**, 387 (2000).

[30] B. Carriere and J. P. Deville, Surf. Sci. **80**, 278 (1979).

[31] C. Zhang, M. A. Van Hove, and G. A. Somorjai, Surf. Sci. **149**, 326 (1985).

[32] (a) S. Tanuma, C. J. Powell, and D. R. Penn, Surf. Interface Anal. **17**, 911 (1991); (b) C. J. Powell and A. Jablonski, Surf. Sci. **488**, L547 (2001).

[33] (a) T. Schroeder, J. B. Giorgi, A. Hammoudeh, N. Magg, M. Bäumer, and H.-J. Freund, Phys. Rev. B **65**, 115411 (2002); (b) A. K. Santra, B. K. Min, and D. W. Goodman, Surf. Sci. **513**, L441 (2002).

[34] Discrepancies in the UPS spectrum of the Mo(112)-$p(2 \times 3)$O surface in this study compared to that reported in Ref. 35 are most likely related to the experimental setup. While in the present study a CMA was used, the data in Ref. 35 were acquired with a hemispherical analyzer. Unlike a CMA that integrates over a non-normal angle with respect to the surface, a hemispherical analyzer detects electrons ejected normal to the surface.

[35] T. Schroeder, J. Zegenhagen, N. Magg, B. Immaraporn, and H.-J. Freund, Surf. Sci. **552**, 85 (2004).

[36] H. Ishii, S. Masuda, and Y. Harada, Surf. Sci. **239**, 222 (1990).

[37] M. Brause, D. Ochs, J. Günster, T. Mayer, B. Braun, V. Puchin, W. Maus-Friedrichs, and V. Kempter, Surf. Sci. **383**, 216 (1997).

[38] T. H. Di Stefano and D. E. Eastman, Phys. Rev. Lett. **27**, 1560 (1971).

[39] B. Fischer, R. A. Pollak, T. H. Di Stefano, and W. D. Grobman, Phys. Rev. B **15**, 3193 (1977).

[40] H. Ibach and J. E. Rowe, Phys. Rev. B **10**, 710 (1974).

[41] F. G. Bell and L. Ley, Phys. Rev. B **37**, 8383 (1988).

[42] A. Di Pomponio, A. Continenza, L. Lozzi, M. Passacantando, S. Santucci, and P. Picozzi, Solid State Commun. **95**, 313 (1995).

[43] K. T. Queeney, M. K. Weldon, J. P. Chang, Y. J. Chabal, A. B. Gurevich, J. Sapjeta, and R. L. Opila, J. Appl. Phys. **87**, 1322 (2000).

[44] C. T. Kirk, Phys. Rev. B **38**, 1255 (1988).

[45] D. W. Berreman, Phys. Rev. **130**, 2193 (1963).

[46] B. Harbecke, B. Heinz, and P. Grosse, Appl. Phys. A **38**, 263 (1985).

[47] At a normal angle of incidence ($\theta_i=0$), transverse waves such as IR photons on a SiO_2 thin film, excite only the transverse optical phonon modes at the surface (Refs. 45–47). However, in case of a *p-polarized* IR beam, both transverse (TO) *and* longitudinal (LO) optical phonon bands are excited if the incidence is *oblique* ($\theta_i \neq 0$) (Ref. 45). As originally explained by Berreman, this effect is due to the perpendicular electric field component of the *p*-polarized light that generates surface charges leading to a resonance at the LO frequencies (Refs. 45 and 46). For a thin film grown on a metallic substrate, the extent of the accentuation of LO modes with respect to TO modes through *p*-polarized, oblique IR light, depends on the film composition (damping of the specific phonon), film thickness, and the angle of incidence (Ref. 46). The thickness at which the intensity of the LO modes is maximized with the concurrent minimization of TO modes is defined as the *Berreman thickness* (Ref. 46). For a-SiO_2 films grown on a metallic substrate, the Berreman thickness is ~50 nm (Ref. 46).

[48] (a) S. Wendt, M. Frerichs, T. Wei, M. S. Chen, V. Kempter, and D. W. Goodman, Surf. Sci. **565**, 107 (2004); (b) J. T. Yates, Jr., *ibid.* **565**, 103 (2004).

[49] M. L. Colaianni, J. G. Chen, W. H. Weinberg, and J. T. Yates, Jr., Surf. Sci. **279**, 211 (1992).

[50] P. K. Stefanov and Ts. S. Marinova, Surf. Sci. **200**, 26 (1988).

[51] T. Sasaki, Y. Goto, R. Tero, K. Fukui, and Y. Iwasawa, Surf. Sci. **502–503**, 136 (2002).

[52] D. A. Muller, T. Sorsch, S. Moccio, F. H. Baumann, K. Evans-Lutterodt, and G. Timp, Nature (London) **399**, 758 (1999).

[53] A. L. Ivanovskii, Russ. J. Inorg. Chem. **46**, S15 (2001).

[54] This observation is fully consistent with that reported in Ref. 15, although Schroeder *et al.* found this shoulder at ~5.2 eV after annealing a SiO_2/Mo(112) surface at 1250 K for 30 min.